

SIMILITUDE MODEL EXPERIMENTS TO DETECT MINE CAVITIES ¹

F. Ziaie
S. S. Peng

and

P. M. Lin ²

Abstract. A resistivity technique for cavity location has been developed. This technique is a combination of the Bristow arrangement and line electrode method. In this technique three line electrodes are used so that the sinkhole electrode is placed far from the other two electrodes. When one of the two electrodes and the sinkhole electrode are activated, several resistivity profiles parallel and perpendicular to the line electrode are measured for different electrode activated. Subsurface cavities cause resistivity anomalies if they are crossed by the resistivity profiles. The anomalies are interpreted and used to locate the sources of the anomalies (cavities). A tank model and a similitude model are developed to verify the effectiveness of this method for cavity detection in the saline medium and in the actual materials. The results of the experiment indicate that the location and the dimensions of the., cavities can be estimated successfully.

Additional Key Words: electrical resistivity, monopole, mine cavity, tank model, similitude model.

¹ Paper presented at the 1990 Mining and Reclamation Conference and Exhibition, Charleston, West Virginia, April 23-26, 1990.

² F. Ziaie, S. S. Peng, and P. M. Lin are Graduate, Charles T. Holland Professor and Chairman, and Research Associate, respectively, at Department of Mining Engineering, College of Mineral and Energy Resources, West Virginia University, Morgantown, WV 26506.

Introduction

Abandoned mine cavities, especially those that are shallow, are an important source of surface instability. Therefore, such cavities should be detected and stabilized to protect the surface establishments. The earth resistivity technique is relatively inexpensive and has shown a high degree of success in locating subsurface cavities. One of the methods used for locating cavities is the tri-potential method of earth resistivity prospecting developed by Carpenter and Habberjam (1955). Later, Habberjam (1969) conducted an extensive study by

analyzing theoretical consideration of this method for locating the cavities by using a brine tank modeling experiment. The monopole resistivity technique originally discussed by Logn (1954), and applied to cavity location by Bristow (1966), was eventually modified by Bates (1973). This technique was employed by the U.S. Bureau of Mines to locate abandoned mines and delineate the boundaries of old workings (Burdick et al. 1986). The line electrode resistivity technique which was modified using the Bristow resistivity arrangement was introduced by Ziaie et al. (1989). This technique was used in a brine tank model experiment in order to test its effectiveness in cavity location.

Discussion of the new technique

The proposed line electrode resistivity technique is analogous to the Bristow monopole configuration. In this method line electrodes are used instead of point electrodes. The point potential electrodes are used within or outside of the two active line electrodes to measure the potential gradient variation generated by the line electrodes. This potential variation is related to the subsurface structure. The major difference between this technique and the Bristow array is that the distribution of the potential in the subsurface delineates revolution of the half cylindrical surfaces rather than spherical surfaces. The axis of these surfaces are correlated with the closest line electrode when the two active electrodes are sufficiently far from each other (Fig. 1). If the subsurface structure does not vary laterally, then the intersections between the cylindrical surfaces and the earth surfaces are parallel equipotential lines. This equipotential gradient is monitored and is used to calculate the resistivity of the subsurface material. In the case of locally lateral variation of the subsurface material (such as the existence of mine cavities) the equipotential line will be distorted and the anomaly due to lateral variation of the subsurface can be interpreted to locate the source of the anomaly. The major advantage of this technique is that (1) the resultant anomaly for different profiles parallel and perpendicular to the line electrode can be monitored simultaneously without the transmission of the line electrode, (2) the detected anomalies can be used to evaluate the cross sectional dimensions of the cavity for the profiles parallel and perpendicular to the line electrodes, and (3) the resolution is appear to be higher than Bristow technique. Therefore, the extension of the cavity in those profiles perpendicular to the line electrode can be measured. The mathematical relation of the potential distribution and subsurface apparent resistivity is available elsewhere (Telford et al. 1976) i.e.

$$\rho_a = \frac{T\pi(L^2 - x^2)}{4 dL} \left(\frac{\Delta V}{I} \right) \quad (1)$$

where L is the half spacing of the two line electrodes (ft.) and x is the distance of midpoint of the two line electrodes from the midpoint of potential electrodes (ft.), d is the half spacing of two potential electrodes (ft.), I is the electrical current delivered to the earth (amps), V is the measured voltage (volts), T is the length of the line electrode (ft.), and ρ_a is the apparent resistivity (ohm-ft).

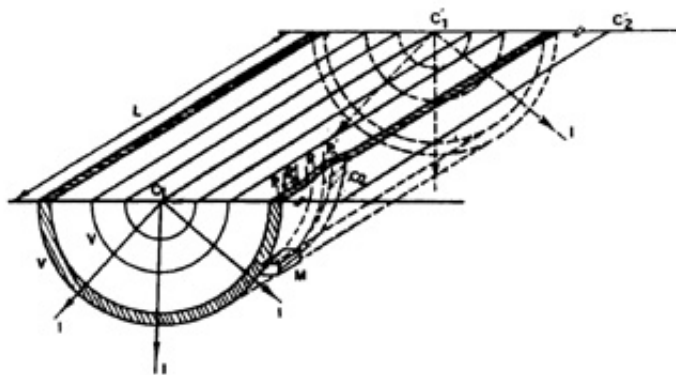


Fig. 1 Distortion of equipotential lines due to crossing of the cylindrical surfaces through a cavity. $C_1C'_1$ and $C_2C'_2$ are line electrodes and $P_1P'_1, P_2P'_2, P_3P'_3...$ are potential electrodes, M is a mine cavity.

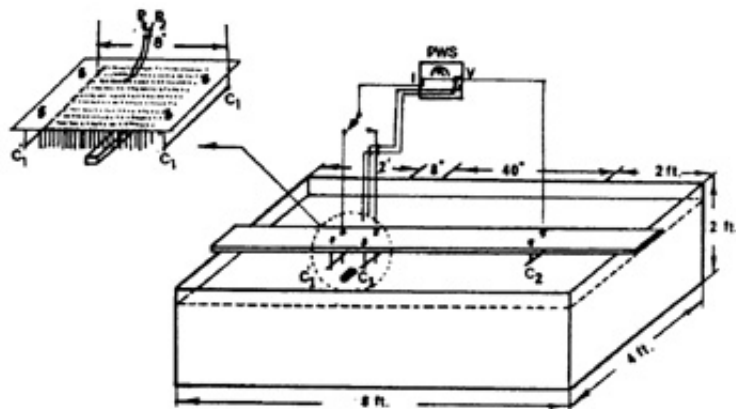


Fig. 2 Tank model.

Plotting of the resistivity anomalies and their interpretation. In this resistivity survey, the measured resistivity is associated with the stations located between the two potential electrodes. Thus for C_1C_2 electrodes activation the resistivity of all the stations are plotted versus their distances from the nearby activated line electrode. Since the same profile is used to measure the resistivity related to the other two activated line electrodes ($C'_1C'_2$), the resistivity values of the same stations are plotted against their distances from the new activated current line electrodes repeatedly. The two profiles are superimposed on each other to obtain a combined profile for interpretation purpose. The potential electrodes spacing used for all the experiments was 0.25 inches and the minimum distance of the potential electrode from the current line electrode was 1.25 inches. The total length of each profile. was 8 inches.

According to the resistivity response analysis of this type of experiments, $2/3$ of the maximum peak anomaly response value associated to the cavity is used for the interpretation purpose. Therefore, a horizontal line from $2/3$ of the maximum amplitude is drawn to intersect the anomaly curve at two adjacent points. The trajectories of the intersected points on the $C_1C'_1$ line are used to draw the appropriate arcs. The arcs are centered at the related activated line electrode. Their radii are the distances of the mentioned trajectory points from the nearby activated current line electrode. The intersections of the two pairs of arcs involved in

any activated current line electrodes delineate the boundary of the detected cavity. The circumscribed square or circle within the intersected area shows the cavity location and dimension (refer to Figs. 4 and 5).

Room and pillar simulation in the tank model experiment. A brine tank, 8 feet long, 4 feet wide and 2 feet high, was designed (Fig. 2). Three current line 7 inch long electrodes were set up as shown in Figure 2. The survey area, 5 inches wide and 8 inches long, was located between the two current line electrodes, C'_1 , and C_1 . The potential electrodes with a spacing of 0.25 inches were moved within the survey area perpendicular to the line electrode. Four simulated square rooms 1 inch wide and 0.76 inches high with spacing of 1 inch were used and placed 1 inch deep in the survey area (Fig. 3). Along the length of the survey area, 22 profiles labeled A, B, C ... V were spaced 0.25 inches apart for measuring the resistivity profiles perpendicular to the line electrodes. Along the width of the survey area 10 profiles labeled 1, 2, 3 ... 10 with spacing of 0.50 inches were also chosen in order to enable measurement of another set of resistivity profiles (Fig. 3). The current line electrodes C'_1 and C_2 were activated and data were acquired in sequential order for profiles 1-1 to 10-10. Similarly, C_1 and C_2 line electrodes were activated and profiles 1-1 to 10-10 again were obtained.

Figure 4 shows the results of the calculation and plotting of the resistivity of the cross-section profile 3-3 which traversed the rooms. The broken line indicated the location of the detected rooms and pillars. The solid line shows the actual location of the rooms and pillars. Figure 5 shows the cross-section profile 7-7 and the result of the interpretation. The actual locations of the rooms are in good agreement with the location of those detected. Other cross-sections parallel to the line electrode (Figs. 6 and 7) were used to estimate the extension of the rooms in a direction parallel to the line electrodes. As shown in Figure 7 the detected extensions of the rooms are quite close to the actual length of the rooms. The solid line shows the detected length of the cross-section of the rooms and the broken line shows the actual length of the cross-section of the rooms. Therefore the height, width, length, and depth of the overburden for the detected rooms are fairly close to their actual location and dimension. Figure 8 shows the resistivity block diagram related to the room and pillar for C_1C_2 activation. This figure shows the resistivity anomaly response for the survey area. The four peak anomalies are related to the four rooms, and the anomaly amplitude diminishes when it is far from the rooms.

Similitude model study of cavity detection. The dimensions of the model are 8 feet long by 4 feet wide (Fig. 9). The very bottom layer or the sandstone layer consists of sand, lime and cement, in proportions of 20:4:1. The second layer consists of rock dust, lime and cement and the proportions of the material used are 10:3:1. The next layer contains very fine-grained coal, lime and cement. The subsequent layer on top of the coal layer is a limestone layer which consists of only lime. On top of this limestone layer is another layer which consists of sand and cement. The proportions of the material used are 5:1. Figure 9 shows the structure and sequences of the five layers used for the similitude model. For all the layers the most important factor is the resistivity property of the materials in each layer of the structure. Other factors such as the Poisson's ratio or elastic modulus were not important in these experiments. Actually, this simulation was designed to demonstrate the resistivity contrast between different layers and to examine how different layers affect the accuracy of the experiments results. Analogous to the tank model three line electrodes were used. The electrode setup was the same as the first experiment. This experiment was conducted to

verify the characteristic curve of resistivity for the five layer structure without cavity creation in the similitude model. Figure 10 shows the view of the survey site. Figure 11 shows the resistivity of cross-section 8-8 stations located between midpoint of the potential electrodes versus their distance from C_1C_2 activated line electrodes. This resistivity curve is consistent with the characteristic curve of multiple layers. As shown, the apparent resistivity in this profile (- begins with the sandstone layer-, increases in the limestone layer and then decreases in the coal layer as depth of the penetration of the injected current in the medium increases. For the rock dust layer, the apparent resistivity may be somewhere between the coal and sandstone layer because there is no apparent changed for, this layer-. Finally, the curve terminates with an increasingly apparent resistivity for the bottom sand layer. This type of curve is generated because the relative resistivity of the sandstone layer is less than the apparent resistivity of the limestone layer, but is higher than the apparent resistivity of the coal layer, The relative resistivity of the coal layer is also less than that of sand or rock dust layer. Therefore, the resistivity profile can provide an idea regarding the structure of the subsurface layers.

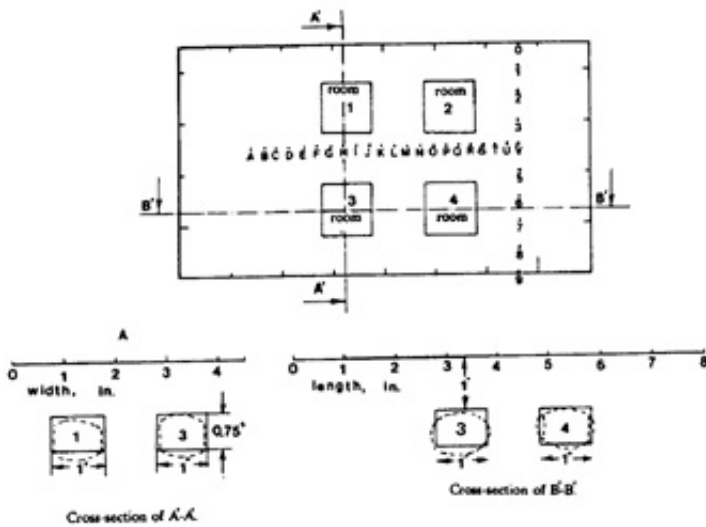


Fig. 3 Location of simulated rooms in the tank model.

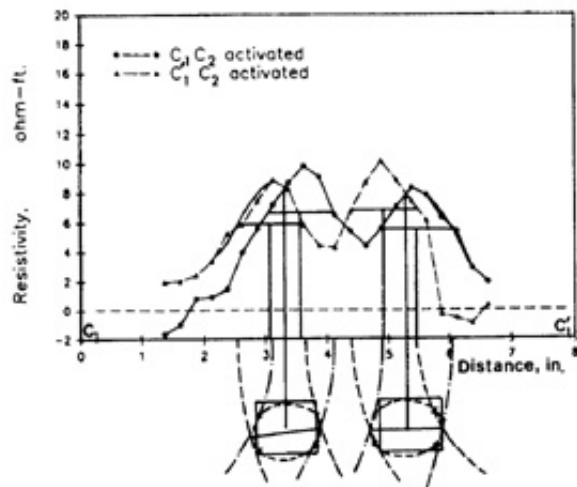


Fig. 4 Interpretation of the resistivity profile for cross-section 3-3.

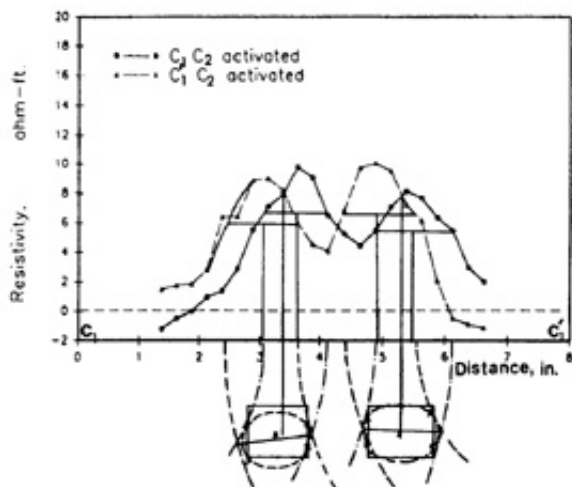


Fig. 5 Interpretation of the resistivity profile for cross-section 7-7

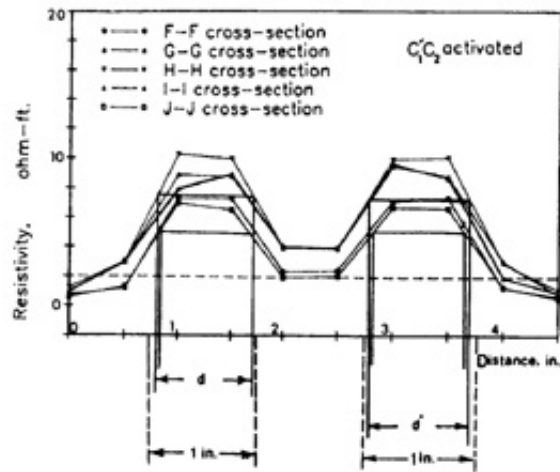


Fig. 6 Interpretation of the resistivity profiles for cross-sections parallel to the line electrodes.

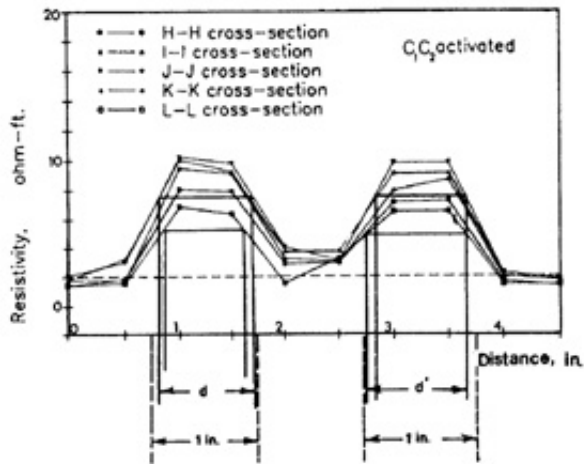


Fig. 7 Interpretation of the resistivity profiles for cross-sections parallel to the line electrodes.

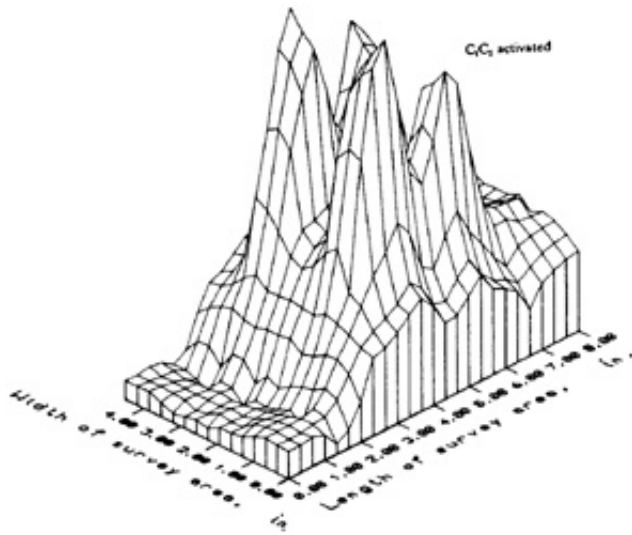


Fig. 8 Block diagram of measured resistivity for 1" depth room and pillar simulation.

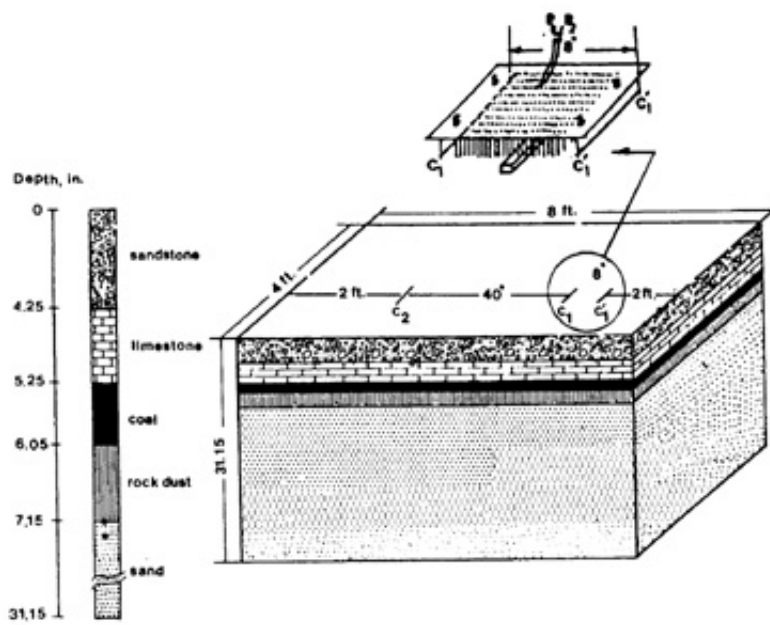


Fig. 9 The similitude model.

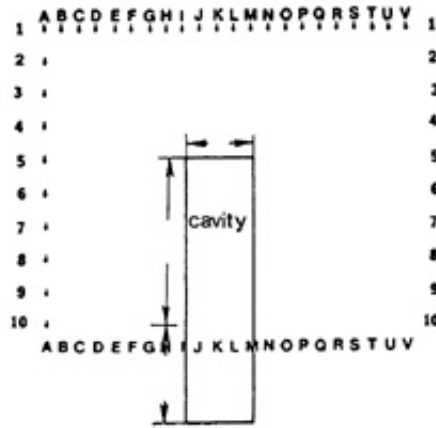


Fig. 10 Location of the created cavity within the survey area in the similitude model. The size, location, and depth of the cavity vary for any experiment.

The next experiment was conducted to detect a circular cavity with a diameter of 0.70 inches that was located at a depth of 1.25 inches (Fig. 12 shows the cavity creation in the model). In the similitude model the resistivity profiles for the cross-section 8-8 was prepared (Fig. 13). The depth of the cavity was 1.30 inches in the sandstone layer, The two -Anomaly curves for different activation of line electrodes C_1C_2 and C'_1C_2 were plotted versus the distance of the midpoint of the potential electrode. For this type of the experiments started from one 3/4th of the maximum amplitude was used for drawing the horizontal line for interpretation purpose rather than 2/3 ratio used in the tank model experiments. The anomaly was interpreted and the predicted cavity is shown in broken line and the actual cavity in solid line. The location of the actual cavity and the detected one is close. The height of the cavity was estimated very closely to the actual one, but the width of the detected cavity was slightly overestimated. The calibration of the response anomaly related to the cavity dimension was practiced initially in order to be applied for anomaly interpretation of different resistivity profiles. Figure 14 shows the result or an anomaly response and the corresponding interpretation and locating of another cavity with a diameter- of 0.20 inches which was located fit a depth of 1.40 inches. In this case the detected cavity was found to be slightly deeper than its actual location. Also, the. width of the cavity was overestimated slightly. The detectability ratio in this case was 7.0.

Finally, a cavity was created at a depth of 2.25 inches with a diameter of 0.20 inches. The profile of the cross section 8-8 is shown in Figure 15. The detected cavity is shown in broken line and the actual cavity in solid line. It is clear that the size and location of the cavity is in good agreement with the size and location of the actual cavity. The ratio of detectability was 11.5 in this experiment.

Conclusion

The new technique of cavity location appears to be applicable for cavity detection in experimental study either in the brine tank model or similitude model. The dimension and the depth of the cavity can be estimated by this technique within certain limits. This technique also provides some ideas related to subsurface structure as well.

Acknowledgement

This project was supported by the U.S. Bureau of Mines under Contract No. J0178030. The opinions expressed here are strictly the authors.

References

- Bates, E. R. 1973. Detection Of subsurface cavities. U.S. Army Waterway Experiment Station Miscellaneous Paper. 5-73--40: 63 p.
- Bristow, C. 1966. A new graphical resistivity technique for detecting air filled cavities. Study in Speleology 1(4): 204 277.
- Burdich, R. G., L. E. Snyder, and W. F. Kimbrough. 1986. A new method for locating abandoned mines. U. S. Bureau of Mines RI 9050: 27.
- Carpenter, E. W. and G. M. Habberjam. 1955. A tri-potential method for resistivity prospecting Geophysics. 21:455-470.
- Habberjam, G. M. 1969. The location of spherical cavities using a tri-potential resistivity technique Geophysics 34(3):780-784.
- Logn, O. 1954. Mapping vertical discontinuities by earth resistivities Geophysics 19.739-760.
- Peng, S. S. and S. M. Hsiung. 1988. Development of guidelines for stabilizing and monitoring the effectiveness of abating subsurface prone area over AML. Annual report submitted to U. S. Bureau of Mines (contract no. J0178030):63.
- Telford, W. M., L. P. Geldart, and R. E. Sheriff. 1976. Applied Geophysics, Cambridge University Press, 860 p.
- Ziaie, F., S. S. Peng, and S. M. Hsiung. 1989. Experimental study of line electrode method to detect underground cavities. p. 369-376. Rock Mechanics as a Guide for Efficient Utilization of Natural Resources. Edited by A. W. Khair, A. A. Balkema publishers.

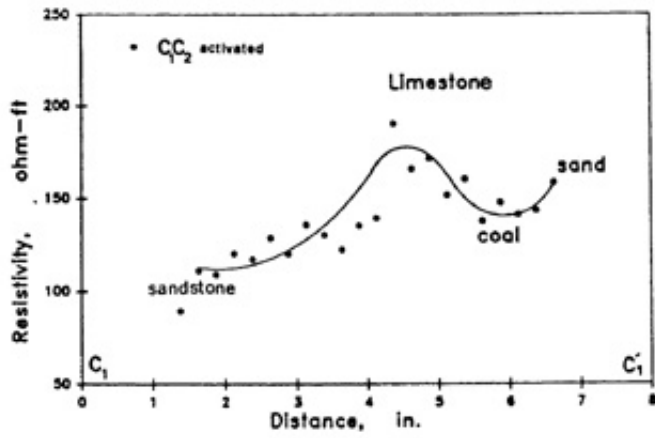


Fig. 11 Resistivity curve of the similitude model.

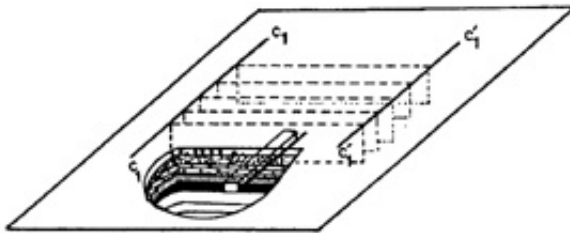


Fig. 12 Cavity creation in the similitude model.

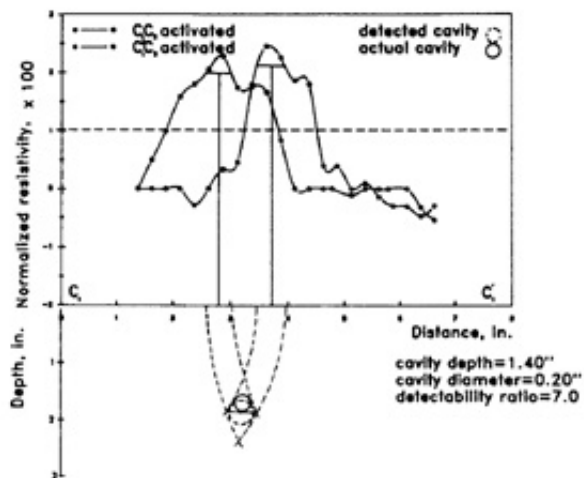


Fig. 13 Resistivity profiles for cross-section 8-8 when the cavity is located at 1.40" depth.

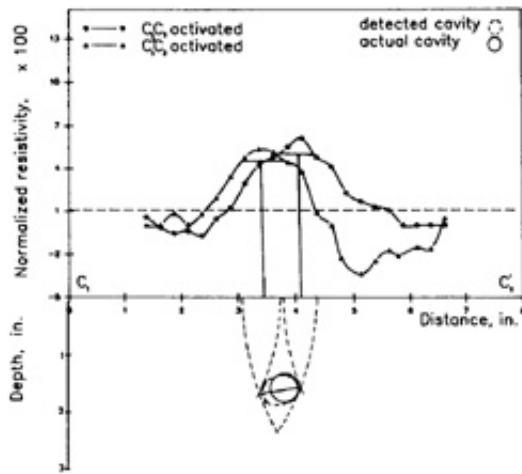


Fig. 14 Resistivity profiles for cross-section 9-9 when the cavity is located at 1.25" depth.

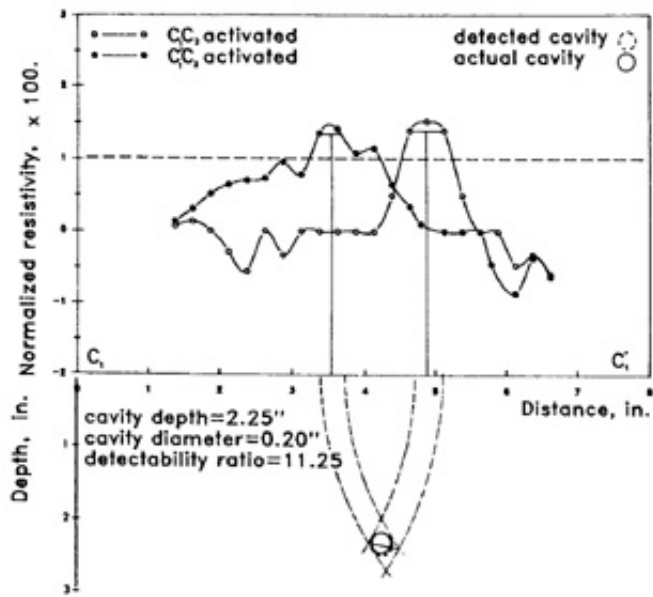


Fig. 15 Resistivity profiles for cross-section 8-8 when the cavity is located at 2.25" depth.